Radio-loud quasars in distant groups and clusters

M.N. Bremer[1], J.C. Baker[2]

[1] Institut d'Astrophysique de Paris, 98bis Bvd Arago, 75014 Paris, France
[2] MRAO, Cavendish Laboratory, Madingley Road, Cambridge CB3 0HA, UK

Abstract

We describe the first results from a programme to search for distant groups and clusters of galaxies using Molonglo radio-loud quasars at $z > 0.5$. We use two techniques to isolate group and cluster members. Firstly, we carry out multicolour imaging of quasar fields in order to search for the old, red, members. Secondly, we carry out sensitive narrow-band imaging to search for redshifted [OII] emission from late-type galaxies at the quasar redshift. Two systems at $z > 0.7$ discovered using these techniques are discussed. One is a compact group of galaxies, apparently at the edge of a larger group, and the other is a cluster centred on a quasar.

1 Introduction

Few *bone-fide* clusters or groups are known at redshifts above $z = 0.7$. Current and past X-ray missions have the sensitivity to detect the most luminous (massive) clusters to this redshift, but not much higher (e.g. see Luppino & Gioia 1995, Rosati et al. 1998). Multi-colour optical surveys (e.g. Postman et al. 1996, Lidman & Peterson 1996), have to cover large areas (many square degrees) in order to find many distant clusters and are therefore inefficient at finding them. The choice of filters in these surveys limit the redshift range they can probe, as the best contrast between a distant cluster and the field occurs when the filters used straddle the 4000 Angstrom break of the older ellipticals in the cluster. The efficiency of these kinds of surveys will improve with the new large-area CCD mosaic cameras available at several telescopes (e.g. the UH8k, Metzger et al., 1995, and Megacam on the CFHT, Hora et al. 1994). These will still suffer from the limitations introduced by the filters used. Moreover, both X-ray and large-area optical surveys are sensitive only to the highest mass sys-

tems at high redshift, they cannot probe correlations with the mass of systems at high redshift.

Consequently, the most efficient way to look for groups and clusters at high-redshift is to use distant markers. Quasars are ideal pointers as they can be seen out to the highest redshifts, and low-redshift work ($z < 0.7$) has shown that radio-loud quasars tend to favour clustered environments (e.g. Yee & Green 1987). Moreover, as quasars are thousands of times more common at $z = 2$ than in the local universe, the discovery of clusters or groups around even a small fraction of them will severely constrain theories of structure formation. However, until now, very little work beyond the detection of clusters from excess number counts around quasars has been carried out.

We have started a project to image the environments of Molonglo quasars in order to find and study distant groups and clusters. The Molonglo quasars are drawn from the sample of Kapahi et al. (1998) and Baker (1994), some hundred radio loud quasars with 408 MHz radio flux of S_{408} >0.95 Jy, taken from the region $-30 < \delta < -20$ and $|b| > 20°$. Our eventual aim is to determine the environmental properties of a representative subset of these quasars, in order to find distant clusters and to determine if there are correlations between the environment and the properties of the quasar. In our work, we try to identify individual group or cluster members, not simply determining a statistical overdensity of objects around the quasar based on single waveband information. We do this for two reasons. Firstly, at $z > 0.7$ only the richest clusters are reliably detected as a statistical overdensity and secondly, the quasars are not necessarily at the centre of the galaxy distribution in a cluster or group, even if they are at the centre of the gravitation potential. Indeed, this is true for the radio galaxy Cygnus A at $z = 0.05$ (Owen et al. 1997); at higher redshifts this situation becomes more common because of the increased frequency of subcluster mergers.

We search for cluster galaxies using two complementary methods. Firstly, we exploit the fact that the ellipticals in the densest part of groups and clusters have a tight colour-magnitude relationship, by imaging the fields of quasars in two bands, one either side of the 4000 Å break at the redshift of the quasar. Ellis et al. (1997) have shown that cluster ellipticals at $z = 0.5$ have a narrow range in rest-frame $U - V$ colour, typically 0.2–0.3 magnitudes. The colours imply that the galaxies have been passively evolving since $z > 2$, so we are able to search for dense cluster cores and compact groups out to $z \sim 1.5$ by looking for clumps of faint, red objects with very similar colours. Moreover, given that the galaxies will have colours comparable to passively evolving systems, we already have an idea of what colour to expect, given the quasar redshift.

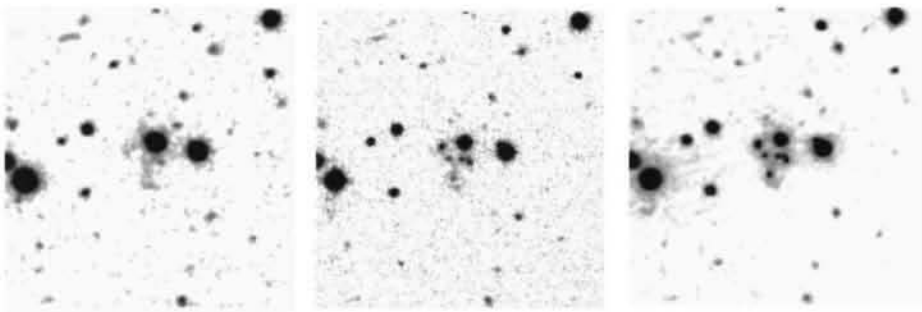

Figure 1. B, R and I-band images of the immediate environment of MRC0941-200. The width of each image is 60″. The quasar is at the centre. South of the quasar, but within 15 arcsecs of it, are five galaxies embedded in "fuzz". The galaxies are considerably redder than the fuzz, they are not visible in the B-band image.

Rakos & Schombert (1996) have shown that at $z > 0.5$ the majority of galaxies in a cluster may be blue star-forming galaxies, and so for a more complete picture we need to identify these as well. To this end, we use the Taurus Tunable Filter (TTF) on the AAT to carry out sensitive narrow-band imaging of the quasar field, to search for line emission from star-forming cluster galaxies.

In the following sections we summarise work on two systems we discovered using the above methods. These are drawn from the first five quasar fields that we observed.

2 MRC0941-200

This quasar is at $z = 0.715$. We imaged the field around it in R, i, J and K with the ESO 2.2m and also in B and I with the CTIO 4m. Figure 1 shows the immediate field of the quasar. The quasar is just to the north of a compact group of galaxies that are surrounded by fuzz. By eye, the fuzz is bluer than the galaxies as only the fuzz remains in the $B-$band image. The fuzz seems to trace the region between the galaxies in the group. The radio emission from the quasar is aligned roughly north-south. The southern radio arm is aligned on the sky with the fuzz, and is considerably shorter than the northern arm (12 arcsec as opposed to 36 arcsec).

We used Sextractor (Bertin & Arnouts 1996) to obtain isophotal magnitudes of objects in the R and i frames. The apertures were defined on the i-band

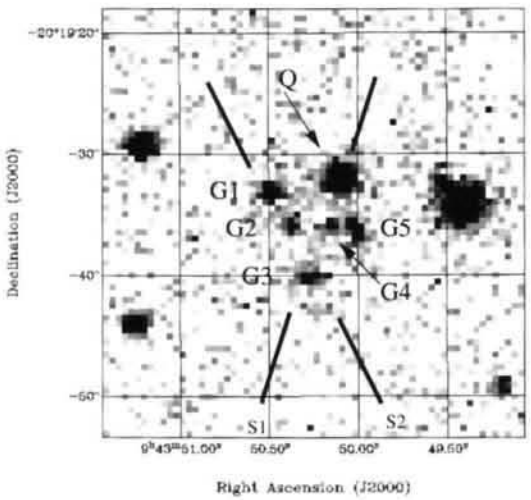

Figure 2. J-band image of the quasar and group with the slit positions used for spectroscopy overlaid. Note that the fuzz between the galaxies is still visible in this band. Similarly, it is also visible in the K'−band image.

frame; at a minimum they had to contain 5 connected pixels (an area of just over 0.5 arcsec^{-2}) brighter than a surface brightness level of 24 mags arcsec^{-2}. This led to a source list complete to about $i = 22.5$, with the faintest detected object having $i \sim 24.2$. We only considered sources brighter than $i = 22.0$ in the analysis. The R and i bands straddle the 4000 Å break of objects at the same redshift as the quasar. All 5 objects close to the quasar had $R - i = 1.15 \pm 0.1$, indicating that they were at the same redshift, and approximately of the same age. This is the colour expected for a passively evolving, old stellar population at the redshift of the quasar.

Spectroscopy of four of the galaxies in the group show that they are at the redshift of the quasar (Figure 3). Two galaxies have [OII] and [OIII] line emission, while all show breaks at around 6900-7000 Å, consistent with 4000 Å breaks at the redshift of the quasar. The spectra also show that the region between the galaxies is filled with ionized gas (emitting in [OII] and [OIII]). Given that the [OII] line is much stronger in the second spectrum towards the southernmost galaxy than towards the easternmost, it seems likely that the line emission traces the same region as the fuzz. All of this indicates that the quasar

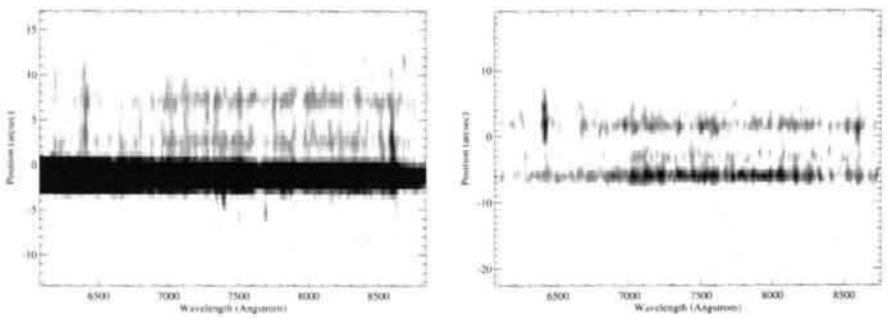

Figure 3. Left. Long slit spectrum through the quasar and the southernmost member of the group (Slit position S1, galaxies G3 and G4 are in the slit). Right. Longslit spectrum through galaxies G1,G2 and G3, slit position S2. The emission-line at 6400Å is [OII], lines at $\sim$ 8500 are the [OIII] doublet. South is to the top in both spectra

is in a compact group of galaxies at $z = 0.715$. The five red galaxies have $R = 21 - 22.5$ and $R - K = 4.4 - 5.0$ (with errors of 0.3 mags), again consistent with old stellar populations at z=0.715.

2.1 The compact group

How does this compact group relate to those found at low redshift? The group satisfies the criteria to be a Hickson group (e.g. see Hickson 1997), the galaxies have luminosities of L* or above, and the average distance between the galaxies is about 25 kpc (for $H_0 = 50$ and $q_0 = 0.5$). However, Hickson groups generally do not have large amounts of line-emitting gas between the galaxies (e.g. Rubin et al. 1991) or fuzz that can be seen from the rest-frame UV to the near IR. They can show tidal tails between galaxies but nothing as spectacular as seen here. Compact groups have extended X-ray halos (e.g. Ponman et al. 1996); these are less extensive (extending to a few hundred kpc) and of lower pressure than those found in clusters of galaxies.

The nature of the fuzz is therefore the key to determining the relationship between this high redshift group and low redshift Hickson groups. The magnitudes and colours of the fuzz are difficult to determine because of the presence of the galaxies in all bands except the B-band, and because of the low-surface brightness of the fuzz (small errors in the value of the background lead to large errors in fuzz magnitude). The B-band magnitude was determined directly by placing an aperture around the fuzz seen in Figure 1. For all the other wave-

bands, we scaled the measured surface brightness in regions not dominated by galaxy emission by the area of the region of fuzz in the B-band, to arrive at an integrated magnitude. We cross-checked this by comparing the surface brightness determined in each band to the magnitude of the quasar in that band. The integrated flux from the fuzz was 6 ± 1 percent that of the quasar in the B-band. Its $B - I$ colour was 2 ± 0.5 mags redder than the quasar. The $J - K'$ colour was 0.8 ± 0.5 mags redder than the quasar, the fuzz in K' having an integrated flux 50-150 per cent that of the quasar.

We now consider several origins for the fuzz. Any model has to account for the similar morphology seen for the fuzz between $B-$ and $K'-$bands, and the coincidence with the line emission. It is unlikely that the fuzz is dominated by scattered quasar light. Scattered light should be bluer than the quasar light. If the scatterer is cold gas or dust there should be a scattered broad MgII emission line (our spectroscopy rules this out to the level of a few percent of the nuclear line). The B-band light should also be polarized. Crude B-band imaging polarimetry carried out on the ESO 2.2m places a limit of ~ 10 per cent on a scattered component. No scattering process can account for the high flux in the K'- band. The Thompson depth of the hot gas in a compact group will not be enough to scatter a large amount of nuclear light. Given the presence of strong extended [OII] and [OIII] emission in the region between galaxies, nebular continuum emission will contribute at least some of the fuzz emission in B (Dickson et al. 1994), but little or none at longer wavelengths.

The fuzz could be starlight. No single model of a $z = 0.7$ galaxy fits the colours of the fuzz (e.g. from Bruzual & Charlot 1993, Guiderdoni & Rocca-Volmerange 1988). Nevertheless, given the morphology of the fuzz, it seems likely that the galaxies are gravitationally interacting with each other, stripping both stars and ISM from the galaxies. If the fuzz consists of old stars plus many regions of vigourous star formation in the stripped ISM, then the mix of stellar types may be such that the colours do not correspond to a well-defined type of galaxy. Such a scenario would, however, lead to the same morphology for the fuzz from $B-$ to $K'-$ band (at least at ground based resolution). The extended emission-line spectrum, if interpreted as that of a starburst, implies a star formation rate of the order of 100 $M_\odot$ yr^{-1}, but this is spread over an area of at least 1000 kpc^2. The B-band flux can be converted directly into a luminosity at 2300 Å in the rest-frame, and then into an approximate star formation rate (e.g. Meurer et al. 1997) of several tens of $M_\odot$ yr^{-1}. This surface density of star formation (about 0.1 $M_\odot$ yr^{-1} kpc^{-2}) is more than two orders of magnitude lower than the maximum surface density for starbursts found by Meurer et al (1997), and so is by no means extreme. The [OIII]/[OII]

line ratio is on the low side for a starburst (flux[OIII]/flux[OII] ~ 0.5), but it is seen in some nearby systems (e.g. see Staninska & Leitherer 1996). In this scenario, the difference between this group and the low redshift Hickson groups is that the member galaxies at z=0.7 are still gas rich, and when they interact their ISM is tidally stripped and undergoes a starburst phase. This enriches any surrounding hot gas halo to the metallicity levels seen in nearby Hickson groups. At z=0, this group will appear as an ordinary Hickson group, the fuzz and the extended emission-lines having more or less disappeared as the starburst population fades.

No rôle is mentioned for the quasar in the above. Energetically, none is needed, but the coincidence between the radio structure and the major-axis of the fuzz implies a connection between them. A straightforward explanation of the asymmetry in the radio structure is that the southern radio jet suffers higher ram pressure confinement than the northern jet, as it passes through a considerably denser IGM on the southern side. Icke (this volume) has shown that jet-induced star formation may not work, but perhaps the backflow region of the radio source (which is transonic or turbulent rather than massively supersonic) can mediate star formation. Certainly the fuzz has the rough dimensions of the backflow region; it should be unresolved width-ways if it was coincident with a radio jet. If the extended emission lines are photoionized by the quasar, then the [OIII]/[OII] line ratio (proportional to the ionization parameter) is lower than most line emission seen around 3C quasars at $z < 1$ (see Bremer et al. 1992 and references therein). This implies either that the gas is seeing a relatively low ionizing flux from the quasar, or that the emission-line gas is at higher pressure than that expected for the hot halo of a group: the emission-line gas is not in pressure equilibrium with the hot phase. This is perhaps to be expected if it has been recently stripped from a galaxy, it will be overpressured relative to the IGM of the group. Photoionization by the quasar reduces the estimated star formation rate, but there should still be star formation to explain at least some of the fuzz seen in the rest-frame blue/UV.

2.2 The larger-scale environment

On the larger scale, the Sextractor photometry revealed that there is a clear overdensity of faint ($20 < I < 22$) galaxies to the north-east of the quasar with the same $R - i$ colour as the group members. Figure 4 shows the spatial distribution of detected objects. The quasar position is shown as an asterisk, objects with $R - i = 1.15 \pm 0.1$ as crosses, the rest as dots. As well as the compact group close to the quasar, there is a clear overdensity of objects to

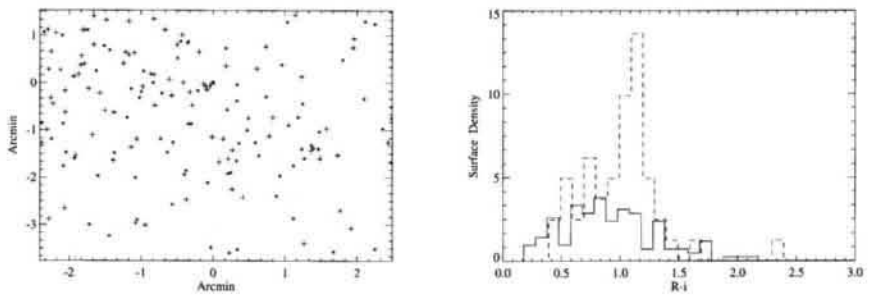

Figure 4. Left: Spatial position of all objects with $20 < i < 22$ detected by Sextractor. Crosses are objects with $1.05 < R - i < 1.25$. Diamonds are objects with 1-σ uncertainties in their colours that allow that color range. Dots represent the rest of the detected objects. Clearly there are more objects with $R - i \sim 1.1$ to the north-east of the quasar (which is shown as an asterisk at [0,0]), than in the rest of the frame. Right: The colour distribution of objects with $20 < i < 22$ in the frame. The dashed histogram is the distribution of colours of objects to the east of the quasar, and the continuous histogram is for objects from the rest of the frame. The difference between the two is dominated by an excess of objects with $R - i \sim 1.1$ to the east of the quasar.

the top left (north-east) with $R - i = 1.15$. A colour histogram (Figure 4) comparing the colour distribution of objects in the north-east to that of the rest of the objects in the i–band frame shows this excess clearly. Given the similar colours of the group galaxies and these objects, a simple explanation is that the compact group is at the edge of a larger structure at the same redshift. If so, then the structure appears more like a loose group rather than a cluster as there seems to be no central condensation of galaxies, or an obvious gE or cD galaxy at the centre. Multi-object spectroscopy is clearly required to determine the reality and nature of this structure.

3 MRC0450-221

This quasar is at $z = 0.898$. It was imaged in V, R and i-bands with ESO telescopes. An overdensity of faint ($R > 20$) red objects ($R - i > 1$) centred on the quasar is obvious indicating that it may be close to the centre of a cluster. We then observed the quasar field with the Taurus Tunable Filter (TTF) on the Anglo Australian Telescope in order to search for candidate [OII] emitters

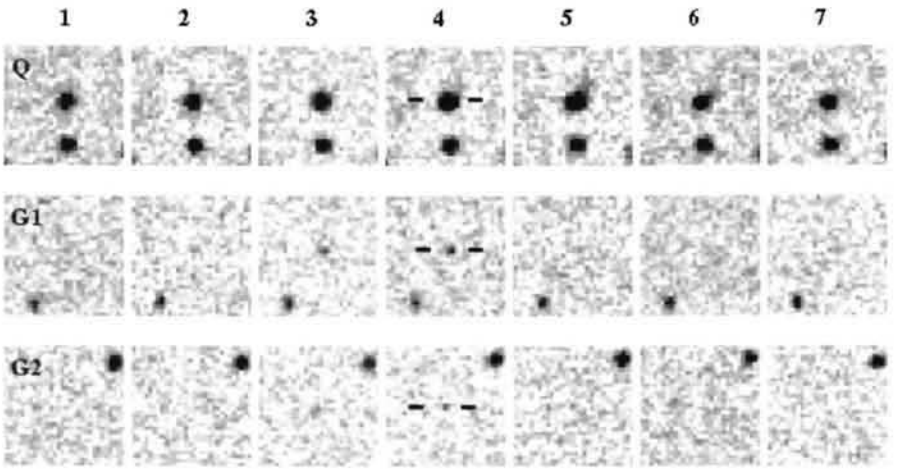

Figure 5. Sub-images drawn from a sequence of seven 1000s TTF images of the field of quasar MRC0450-221 at z=0.898. These are taken using 10Å-FWHM adjoining pass-bands spanning the nuclear [OII] line in the quasar (column 4). Extended [OII] emission is seen around the quasar (Q) up to 1000 km s^{-1} red-ward of the nuclear emission, aligned with the radio axis. Two galaxies (G1 and G2) with redshifts within 500 km s^{-1} of that of the quasar are shown in the bottom two rows. Each sub-image spans about 500 km s^{-1} at the quasar redshift. Column 1 is 1500 km s^{-1} blue-ward of the quasar redshift, column 7 is 1500 km s^{-1} red-ward.

around the quasar redshift.

Seven 10 Å-wide ($\sim$ 500 km s^{-1}) narrow-band images were obtained, stepping in central wavelength from +1500 km s^{-1} to −1500 km s^{-1} through the wavelength of the redshifted [OII] line of the quasar. Each image was made from two 500 second exposures. Figure 5 shows sub-images drawn from the sequence of TTF images of the $10' \times 10'$ field centred on the quasar. Extended line-emission from the quasar (Q) is seen up to 1000 km s^{-1} red-ward of the nuclear redshift. Two emission-line galaxies (G1 and G2) with redshifts within 500 km s^{-1} of the quasar redshift are shown in the bottom two rows.

Average images centred on ($\pm$750 km s^{-1}) and off ($\pm 750 - 1500$ km s^{-1}) the quasar [OII] wavelength were made as a first step in identifying emission-line galaxies at the quasar redshift. Images at the central three wavelength settings (3, 4 and 5 in Figure 5) were combined as the on-band image and the other

images were combined to form the off-band image. A combined total image was made by adding all seven frames together.

Aperture photometry (using a 2 arcsec radius aperture) was carried out on the on and off-band images. This small aperture size optimised the signal-to-noise for our mainly small and faint targets, but required a correction of 0.4 mags (measured from stars in the field) to obtain accurate total magnitudes. A 1σ uncertainty of 0.2 mags at R=21 was determined for the on-band image. A finding list was made from the total image and this list was matched to the on and off catalogues.

Emission-line galaxies were identified on the basis of the above photometry (a range of other photometric techniques were tried, giving consistent results). Eleven candidates fainter than $R = 20$ with off-on magnitude excesses of more than 3σ were detected. (See Figure 6; we expect only one or two from Poisson statistics). These are the objects with more flux in the on-band than in the off-band. Seven objects fainter than $R = 20$ with a negative off-on magnitude difference greater than 3σ were also detected. These are candidates for galaxies with redshifts between 750 and 1500 km s^{-1} blue-ward or red-ward of the quasar. All emission-line candidates were followed up by inspection of the seven individual images to ensure that they really do appear brighter in one or two consecutive bands than in the rest of the images.

Based on the work of Cowie et al. (1997), we expect to see only 1-2 line emitting field galaxies at z=0.9 in the volume surveyed to our detection limit. A few (less than 5) lower redshift [OIII] and Hα emitters should also contaminate our candidate list, but these should be brighter than $R = 20$. Thus we have a clear excess of emission-line candidates over the expected number of field objects. Assuming these objects are at z=0.9, they have observed [OII] equivalent widths of 30-300 Å, implying star formation rates of a few $M_{\odot} yr^{-1}$.

The candidate emission-line galaxies appear to cluster around the quasar, but not as strongly as the red objects detected in the broad-band imaging, with those candidates with high peculiar velocities appearing to be clustered differently from those candidates with redshifts close to that of the quasar. This is perhaps to be expected, if one believes that the emission-line objects have recently fallen into the cluster. The correlation between velocity and position is exactly what is predicted if clusters form from hierarchical mergers of groups and individual in-falling galaxies

Again, all of this needs confirmation with multi-object spectroscopy but, if it is confirmed, then we are detecting subclustering both spatially and in velocity structure.

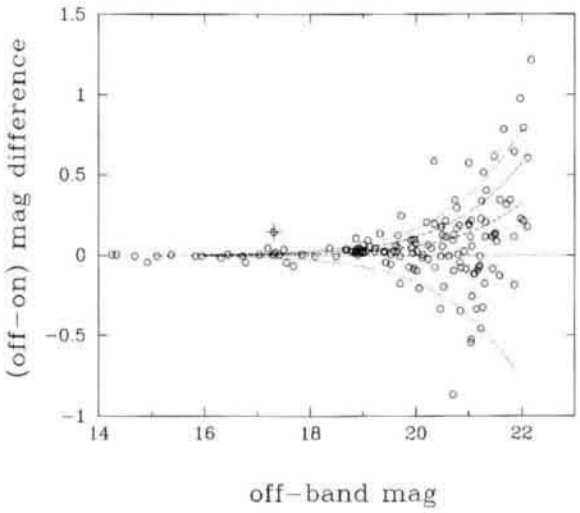

Figure 6. Colour-magnitude plot showing magnitude differences between summed TTF images centred on ($\pm$750km s^{-1}) and off ($\pm$750$-$1500km s^{-1}) the quasar redshift. Signal-to-noise curves ($1, 2, 3\sigma$ and -3σ) are overlaid. The quasar is identified by a cross.

4 Conclusions

The above two examples validate our techniques. The results so far seem to indicate that MRC quasars are in locally clustered environments, even if they are not at the centres of rich clusters. We seem to have detected subclustering both spatially and also in velocity structure, based on the narrow-band work carried out with the TTF. This is exactly what is expected if clusters (and groups) are forming at $z > 0.5$ from mergers of sub-clumps and infall of spiral galaxies. The narrow-band work is vital in all of this, as the candidate emission-line galaxies trace more extended structures than the red galaxies detected by broad-band imaging. At $z > 1$ $J-$ and $K'-$band imaging will become more important in identifying the red group and cluster galaxies. Because the quasars cannot be guaranteed to be at the centre of any structure, relatively wide-field ($5' \times 5'$) IR cameras are required; a $2' \times 2'$ field centred on the quasar may miss the densest parts of a high redshift cluster or group. In this respect a large format camera on a 4m telescope is more useful than a small-format camera on

an 8m.

Acknowledgements We thank our collaborators, Matt Lehnert, Dick Hunstead, Joss Bland-Hawthorn and Peter Barthel. This work was supported in part by the Formation and Evolution of Galaxies network set up by the European Commission under contract ERB FMRX-CT96-086 of its TMR programme.

References

Baker J.C., PhD Thesis, Sydney University
Bertin E., Arnouts S., 1996, A&AS, 117, 393
Bremer , M.N., Crawford, C.S., Fabian, A.C., Johnstone, R.M., 1992, MNRAS, 254, 614
Bruzual G., Charlot S., 1993, ApJ, 405, 538
Cowie L., 1997, ApJ, 481, L9
Dickson R., Tadhunter, C., Shaw, M., Clark, N., Morganti, R., 1995, MNRAS, 273, 29
Ellis R.S., Smail, I, Dressler, A., Couch, W.J., Oemler, A., JR., Butcher, H., Sharples, R.M., 1997, ApJ, 483, 582
Guiderdoni B., Rocca-Volmerange B., 1988, A&AS, 74, 185
Hickson P., 1997, ARA&A, 35, 357
Hora J.L., Luppino G.A., Hodapp K-W, 1994, SPIE, 2198, 498
Kapahi et al, 1998, AJ, submitted
Lidman C., Peterson B., 1996, AJ, 112, 2454
Luppino G.A, Gioia I., 1995, ApJ, 445, L77
Meurer G.R., Heckman, T.M., Lehnert, M.D., Leitherer, C., Lowenthal, J., 1997, AJ, 114, 54
Metzger M.R., Luppino G.A., Miyazaki S., 1995, BAAS, 187, 7305
Owen, F., Ledlow, M.J., Morrison, G.E., Hill, J.M., 1997, ApJ, 488, L150
Ponman T.J., Bourner, P.D.J., Ebeling, H., Bohringer, H., 1996, MNRAS, 283, 690
Postman M., Lubin, L.M., Gunn, J.E., Oke, J.B., Hoessel, J.G., Schneider, D.P., Christensen, J.A., 1996, AJ, 111, 615
Rosati P., Della Ceca, R., Norman, C., Giacconi, R., 1998, ApJ, 492, L21
Rubin V.C., Ford, W.K., JR., Hunter, D,A., 1991, ApJS, 76, 153
Stasinska G., Leitherer C., 1996, ApJS, 107, 661
Yee H., Green, R., 1987, ApJ, 319, 28